

Quantitative Surface Color Measurement of Tomato Fruit Using Illuminating Spectral Information of Natural Lighting

Atsushi Hashimoto*, Ken-ichiro Suehara, Takaharu Kameoka

Graduate School of Bioresources, Mie University, 1577 Kurimamachiya-cho, Tsu, Mie 514-8507, Japan
hasimoto@bio.mie-u.ac.jp

This study aims to develop a quantitative surface color measurement method of agricultural products under natural lighting conditions. We then analyzed the relationship between the color appearance differences of the images taken under the standard and natural lighting conditions based on the illuminating radiance spectral characteristics. Based on the photosensitive characteristics of five kinds of tested cameras, the applicability was studied using the images of tomato fruits whose surface color dynamically changes from green to red. As the results, the RGB values of the images of the red, green, and blue sections on the virtual standard color chart could be calculated using the simple spectral features of the various natural lighting conditions, and consistently agreed with the actual values. In addition, the images of tomato fruits acquired under the natural lighting conditions using the tested cameras were successfully calibrated based on the color parameter differences between the standard color images taken under the standard and natural lighting conditions.

1. Introduction

The rapid, easy, cheap, non-destructive, and non-chemical quality evaluation of agricultural products is one of the most important factors for the sustainable production through the agricultural process. The color of agricultural products is practically and commonly used as a quality index in the agricultural process such as cultivation, harvesting, sorting and packing, since the color could be reflected by the pigment components, which are some of the final components during the primary and secondary metabolic processes, and by the geometrical structure such as the shape and surface conditions. Additionally, the outside appearances of agricultural products could relate to the market price. Moreover, the color evaluation is also a very important index in the agricultural processes using agricultural products such as cassava (Khongsumran et al., 2014) and coffee (Caetano et al., 2013). The objective and quantitative evaluation method with the above qualifications is then significantly desired in many agricultural fields.

There are various machine vision studies regarding the color of agricultural products after certain processes, such as drying (Tatemoto and Michikoshi, 2014) and that have been reported (Abdullah et al., 2006; Brosnan and Sun., 2002). The color measurements using a colorimeter and a digital camera based on the $L^*a^*b^*$ (L^* : lightness variable, a^* and b^* : chromaticity indices) or RGB (R : Red, G : Green, B : Blue) color coordinate system are usually performed for the quantitative color evaluation of agricultural products. We adopted the HSL (H : Hue, S : Saturation, L : Lightness) color system for the color image analysis of the images taken by a CCD camera (Kameoka et al., 1994), since the color analysis had the advantage that it easily and two-dimensionally acquires the surface information and the color distribution (Motonaga et al., 1997).

The color appearance of the image acquired in the agricultural fields is significantly influenced by the illuminating conditions which could be dynamically and continuously changing. Therefore, it is still very difficult to quantitatively evaluate the color appearances of agricultural products. We also studied the quantitative color evaluation method of agricultural products in the agricultural fields (Motonaga et al., 2004). Additionally, we developed the continuous and quantitative remote monitoring method of the surface color changes of agricultural products during cultivation using a digital camera equipped on the Field Server (Fukatsu and Hirafuji, 2005) by analyzing the color parameters of the image compared to the standard color chart

(Hashimoto et al., 2012b). However, the discoloration of the standard color chart for the color calibration was a problem.

We have been evaluating the quantitative color appearance of agricultural products using the illuminating information by analyzing the relationship between the color appearance of the image taken by a digital camera and the illuminating spectral information (Hashimoto et al., 2014). This study aims to develop a quantitative surface color evaluation method of agricultural products based on the generic specifications of digital cameras under natural lighting conditions. We then studied the influences of the sensor elements and the number of pixels on the color evaluation using different types of digital cameras having different specifications. Additionally, the developed method was applied to the tomato images taken under the natural lighting conditions, since the surface color dynamically changes from green to red, and has a complicated color distribution and geometrical structure..

2. Materials and methods

2.1 Materials

The tomato plants (Momotarou) cultivated in a greenhouse located in the Experimental Farm of the Field Science Center of Kii-Kuroshio Life Area, Graduate School of Bioresources, Mie University, Tsu, Japan, were prepared for the experiments. We also made the standard RGB color charts (Hashimoto et al., 2012b) for the color calibration of the images under the outdoor conditions. The standard RGB color chart contains plain red, green and blue sections.

2.2 Methods

The setup of the color image acquisition system (Motonaga et al., 2004; Hashimoto et al., 2012b) is shown in Figure 1. The system is composed of a digital camera, six fluorescent lights at a 5500 K color temperature (TRUE-LITE, DURO-TEST Co., Ltd.) and two diffuse reflectors.

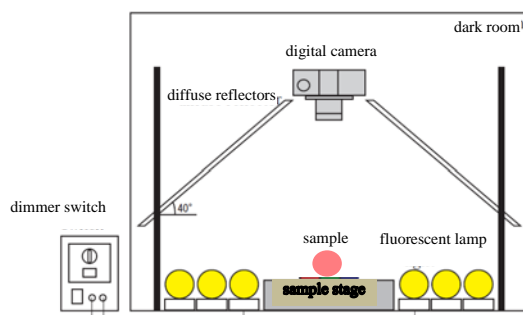


Figure 1: Scheme of standard color image acquisition system.

Five kinds of single-lens reflex digital cameras with different specifications as listed in Table 1 were tested in order to study the adaptability of the quantitative color evaluation method developed in our previous studies (Hashimoto et al., 2013).

Table 1: Specifications of tested digital cameras.

| Cameras | A1 | B1 | B2 | C1 | C2 |
|------------------|---------------|--------|--------|---------|---------|
| Manufacturer | A | B | B | C | C |
| Sensor element | Honeycomb CCD | CMOS | CCD | CMOS | CMOS |
| Number of pixels | 12.34 M | 12.30M | 6.10 M | 15.10 M | 10.10 M |

The use of the TRUE-LITE fluorescent light is based on the CIE (Commission Internationale de l'Eclairage) regulations, and is almost the same as natural lighting since its color rendering index is 91. The light from the light sources is scattered on the diffuse reflectors placed over the light sources in order to prevent any specular reflection on the sample surface. The illuminance adjusted to 140 lx using the white diffuse reflectors and a dimmer switch was treated as the standard lighting conditions in this study. The visible spectral radiance of the lighting ranging from 380 to 730 nm in 10 nm intervals was measured by a spectral measurement

device (Eye-One Prophoto, GretagMacbeth Co.). When the tomato images were acquired, the standard RGB color chart was also placed just behind the tomato fruit.

The images were also taken under the field conditions near the window facing forward in the southwest direction on the 6th floor of the building of the Graduate School of Bioresources, Mie University, Tsu, Japan (north latitude 34.745958333, east longitude 136.522975000). The geometric relation between the camera and the sample under the natural lighting conditions was the same as that for the standard color image acquisition system. However, the lighting conditions, such as the color temperature and the geometric relation between the sample and the light source (the sun), depended on the date, the time and the weather. Figure 2 is an example of the variation in the spectral radiance of the natural lighting.

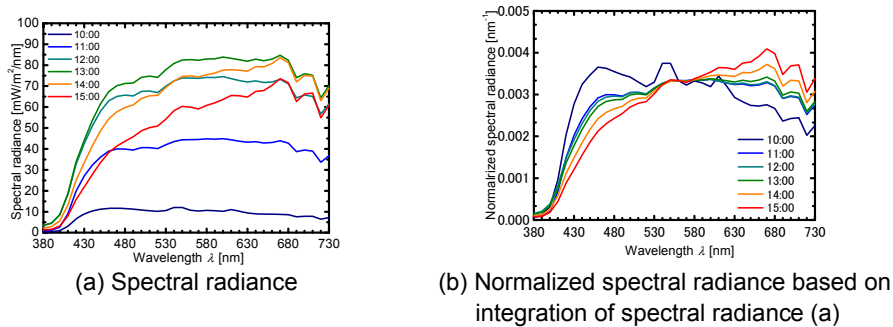


Figure 2: Example of spectral radiance changes of natural lighting over one day.

3. Results and Discussion

3.1 Color appearance characteristics

The difference in the lighting illumination and exposure adjustment of the camera affect the output values of the color parameter on the recorded image. We then studied the influences of the illuminating and the image acquisition conditions on the color parameters of the acquired image in order to understand the characteristics of the digital camera as the detector.

Figure 3 shows examples of the images of the standard color chart and tomato fruits acquired under the standard illuminating conditions using the TRUE-LITE at 140 lx, and represents the influences of the camera specification on the color appearances of the acquired images. The slight color appearance differences among the images were observed though the images were taken under the same acquisition settings.

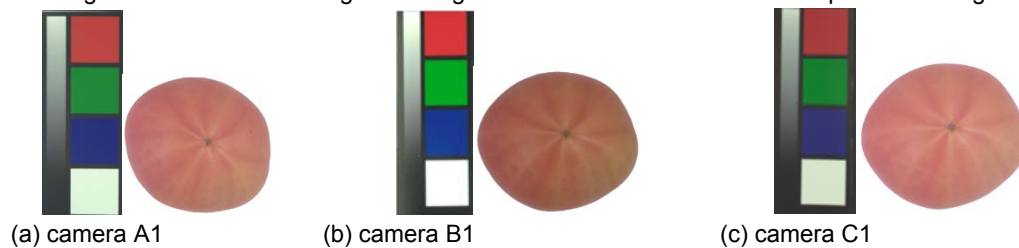


Figure 3: Examples of images acquired under standard illuminating conditions at 140 lx using TRUE-LITE.

In order to understand the color appearance differences, we analyzed the changes in the average R, G or B values of each color section on the standard color chart images taken under the TRUE-LITE illumination using the standard color image acquisition system. The modified focal plane exposure, Hm defined by Eq(1) (Hashimoto et al., 2012a), is related to the photosensitivity of the camera based on the spectral characteristics of the light exposing the standard color chart and the reflectivity of each color section.

$$Hm = \frac{S \cdot T}{F^2} \quad (1)$$

where, F and T are, respectively, the F-number and exposure time of the camera. The value S is the integration of the multiplication of the monochromatic intensity exposing the red, green, or blue section on the color chart and its reflectivity with the wavelength, and is closely related to the optical intensity detected by the camera (Hashimoto et al., 2012a).

All of the RGB values of the images of each color section on the color chart taken under the TRUE-LITE illuminating conditions increased to a decimal power for the Hm values. However, the tendencies of the RGB values to Hm were different for each camera. These results suggested that the curve of the relationship between Hm on RGB values were significantly affected by the manufacturer and the camera specifications. Both the RGB and Hm values were then standardized based on their maximum values of RGB_{max} and Hm_{max} for the analysis of the relationship between them under the various lighting conditions. All of the standardized curves in Figure 4 for all the tested cameras could be simply represented by a power function curve. Additionally, the relationships between the RGB and Hm values were well defined by the power function expressed by Eq(2) with correlation coefficients over 0.993.

$$\frac{RGB}{RGB_{max}} = a \cdot \left(\frac{Hm}{Hm_{max}} \right)^b \quad (2)$$

In Eq(2), the parameters a and b , respectively, could be related to the spectral pattern of the illuminating light and the apparent sensitivity characteristics of the camera as an image sensor. Additionally, the fitting parameter b as the exponent indicated the unique value (0.546) for all the illumination conditions and color sections, and the value was almost the same as that obtained for a specified camera in our previous study (Hashimoto et al., 2013). These results might mean that the R , G and B parameters of the images acquired under a specified condition could be converted into those under the standard lighting conditions at 140 lx using the TRUE-LITE with the white diffuse reflectors.

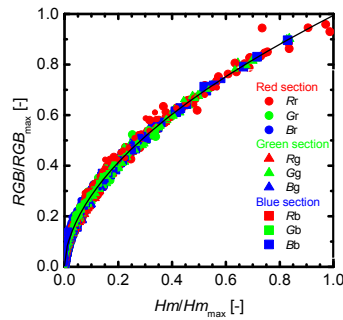


Figure 4: Normalized relationship between Hm and RGB values of images of standard color charts taken by the standard color acquisition system.

3.2 Color calibration based on simple illuminating information

In order to estimate the color parameters of the image taken under a specified condition, we studied the applicability of parameter b obtained in Figure 4. In Figure 5, the R , G and B values of the images of each color section on the virtual color chart estimated using the average b values based on Figure 4 are compared to those estimated using the original b values for the tested cameras, and excellent agreements between them were observed. These results suggest that the parameter b value could be experimentally treated as a constant.

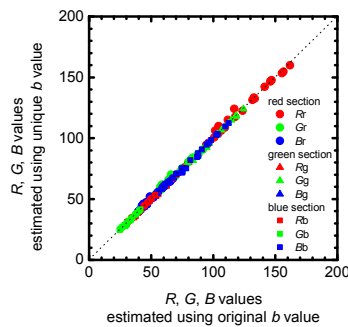


Figure 5: Comparison of color parameters between images of virtual color charts estimated using original and unique b values.

In our previous study (Hashimoto et al., 2012a), we needed the entire spectral information to determine the Hm and a values in Eq(2). However, for application in agricultural fields, it should be easily evaluated using only the simple information of the illuminating characteristics and not the entire spectral information. We could then estimate the Hm values based on the reflected intensities of the illuminating light on the red, green, and blue sections of the color chart at the wavelengths of 490, 550 and 650 nm (ΔS_{490} , ΔS_{550} , ΔS_{650}), respectively, in which the illuminating spectral pattern could be characterized.

In addition, we tried to estimate parameter a by analyzing the spectral pattern changes of the natural lighting (Figure 2(b)) at these wavelengths related to the blue, green and red color, and performed a multiple linear regression analysis using Eq(3).

$$a = \alpha \left(\frac{\Delta S_{650}}{\Delta S_{550}} \right) + \beta \left(\frac{\Delta S_{490}}{\Delta S_{550}} \right) + \gamma \quad (3)$$

We could then calculate the R , G , and B values of each color section on the virtual color chart by estimating parameters Hm and a based on the assumption of the various natural lighting conditions with the unique parameter b .

Furthermore, based on the color parameter differences between the images of the virtual color chart simulated under the natural lighting conditions and the standard one acquired under the standard illuminating conditions at 140 lx using the TRUE-LITE with the white diffuse reflectors, the color calibration developed in our previous study (Hashimoto et al., 2012b) was then performed as follows. The R , G , and B values of each color section on the virtual color chart simulated under which the image acquisition conditions that sample image was taken, C' , could be expressed by multiplying the color transformation matrix A for the color calibration with the color parameter matrix C for each color section on the standard image.

$$C' = A \cdot C \quad (4)$$

$$A = \begin{pmatrix} a_{11} & a_{12} & a_{13} \\ a_{21} & a_{22} & a_{23} \\ a_{31} & a_{32} & a_{33} \end{pmatrix}, C = \begin{pmatrix} Rr & Gr & Br \\ Rg & Gg & Bg \\ Rb & Gb & Bb \end{pmatrix}, C' = \begin{pmatrix} R'r & G'r & B'r \\ R'g & G'g & B'g \\ R'b & G'b & B'b \end{pmatrix} \quad (5)$$

The color calibration image is obtained by multiplying matrix A with the column vector of the R , G , and B values corresponding to each pixel that composes the sample image:

$$\begin{pmatrix} r' \\ g' \\ b' \end{pmatrix} = A \cdot \begin{pmatrix} r \\ g \\ b \end{pmatrix} \quad (6)$$

where, r , g and b are the R , G , and B values of a picture element of the sample image, respectively. r' , g' and b' are the R , G , and B values of the picture element after the color calibration, respectively.

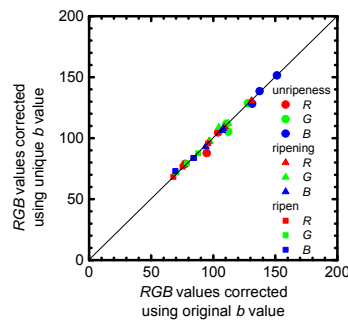


Figure 6: Comparison of color parameters between tomato fruit images calibrated based on virtual color charts estimated using original and unique b values.

In Figure 6, the calibrated data of the tomato fruit images estimated using the average b values taken under the natural lighting conditions are compared to those estimated using the original b values for the tested cameras. The consistent agreements between them are obtained for the images of the unripened, ripening and ripened tomato fruits taken under natural lighting conditions. In our previous study (Hashimoto et al.,

2013), the tomato images were successfully calibrated based on the illuminating spectral information using a specific digital camera. Therefore, these results suggest that the surface color images of the agricultural products with the complicated geometrical structure and color distribution could be quantitatively evaluated based on the simple illuminating information in the agricultural fields.

4. Concluding remarks

By analyzing the relationship between the color appearance of the image taken by several kinds of digital cameras with the different specifications and the spectral feature information, the photosensitive characteristics for all the tested cameras were experimentally represented by a curve, and the relationships between the *RGB* values and *Hm* were experimentally independent of the digital camera specifications and the manufacturers. Additionally, the *RGB* values of the images of the red, green, and blue sections on the virtual standard color chart could be simulated using the simple spectral features of the various natural lighting conditions, and consistently agreed with the actual values. Furthermore, the quantitative color evaluation method could be successfully applied to the images of tomato fruits acquired under the natural lighting conditions. Consequently, this study plays a very important role in developing the surface color analysis for both the simple and rapid evaluations of the plant vigor in agricultural fields and the agricultural research interests.

Acknowledgements

The authors sincerely thank the Idea Scout (IS) Programme of Semiconductor Technology Academic Research Center (STARC) and the Project "Integration research for agriculture and interdisciplinary fields," Ministry of Agriculture, Fisheries and Forests, Japan, for the financial support of this research project.

References

- Abdullah, M. Z., Mohamad-Saleh, J., Fathinul-Syahir, A. S., Mohd-Azemi, B. M. N., 2006, Discrimination and classification of fresh starfruits (*Averrhoa carambola* L.) using automated machine vision system, *J. Food Eng.* 76, 506-523.
- Brosnan, T., Sun, D.-A., 2002, Inspection and grading of agricultural and food products by computer vision system – A review, *Comp. Electron. Agric.* 36, 193-213.
- Caetano, N.S., Silva, V.F.M., Melo, A.C., Mata, T.M., 2014, Potential of Spent Coffee Grounds for Biodiesel Production and Other Applications, *Chem. Eng. Trans.*, 35, 1063-1068.
- Fukatsu, T., Hirafuji, M., 2005, Field monitoring using sensor-nodes with a Web server, *J. Robot. Mechatron.* 17, 2, 164-172.
- Hashimoto, A., Furusawa, K., Suehara, K., Kameoka, T., 2012a, Quantitative color appearance evaluation based on spectral information of natural lighting, In *Proceedings of International Conference of Agricultural Engineering (CIGR-AgEng2012)* (July 8-12, 2012, Valencia, Spain), C1967.
- Hashimoto, A., Furusawa, K., Suehara, K., Kameoka, T., 2013, Quantitative color appearance evaluation of agricultural products based on natural lighting information, *Proceedings of EFITA/WCCA/CIGR VII 2013 Joint Conference* (June 23-27, 2013, Turin, Italy), C0258.
- Hashimoto, A., Suehara, K., Kameoka, T., 2012b, Quantitative Evaluation of Surface color of Tomato Fruits Cultivated in Remote Farm Using Digital Camera Images, *SICE J. Cont. Meas. Syst. Integra.* 5, 18–23.
- Hashimoto, A., Toyoshi, Y., Suehara, K., Kameoka, T., 2014, Quantitative Color evaluation of digital images based on illuminating spectral information, In *Proceedings of 9th Conference of the Asian Federation for Information Technology in Agriculture* (September 29 – October 2, 2014, Perth, Australia), 200-207.
- Kameoka T., Hashimoto, A., Motonaga, Y., 1994, Surface color measurement of agricultural products during post-ripening. In *Color Forum Japan '94 Proceedings* (October 27-28, 1994, Tokyo, Japan), 11-14.
- Khongsumran, O., Intanoo, P., Rangsunvigit, P., Chavadej, S., Leethochawalit, M., 2014, Enhancement of Anaerobic Digestion of Cellulosic Fraction in Cassava Production Wastewater by Microaeration, *Chem. Eng. Trans.*, 39, 553-558.
- Motonaga, Y., Kameoka, T., Hashimoto, A., 1997, Color development of tomato during post-ripening, In *AIC Color 97 (Proceedings of the 8th Congress of International Colour Association)* (May 25-30, 1997, Kyoto, Japan) Volume II, 929-932.
- Motonaga, Y., Kondou, H., Hashimoto, A., Kameoka, T., 2004, A method of making digital fruit color charts for cultivation management and quality control, *J. Food Agri. Environ.* 2, 160-166.
- Tatemoto, Y., Michikoshi, T., 2014, Drying characteristics of carrots immersed in a fluidized bed of fluidizing particles under reduced pressure, *Drying Technol.*, 32, 1082-1090.